ELSEVIER

Journal of Organometallic Chemistry 637–639 (2001) 631–641

Journal of Organometallic Chemistry

www.elsevier.com/locate/jorganchem

Preparation, characterization, electrochemical studies and crystal structure determination of salicylaldehyde–aroylhydrazone, ferrocenyl–aroylhydrazone and salicylaldehyde–ferrocenoylhydrazone complexes of indium

Yaofeng Yuan [a], Zhong Cao [a], Nanyan Fu [a], Jitao Wang [a], Linhong Weng [b], Antonio Bezerra de Carvalho [c], Clovis Peppe [d,*]

[a] *Department of Chemistry, Nankai University, Tianjin 300071, China*
[b] *Institute of Elemento-Organic Chemistry, Nankai University, Tianjin 300071, China*
[c] *Departamento de Quimica, CCEN, Universidade Federal da Paraiba, Campus I, Joao Pessoa PB 58059-900, Brazil*
[d] *Laboratório de Materiais Inorgânicos, Departamento de Química, Universidade Federal de Santa Maria, Campus UFSM, Santa Maria RS 97105-900, Brazil*

Received 12 February 2001; received in revised form 15 March 2001; accepted 10 April 2001

Abstract

The reaction of triethylindium with salicylaldehyde–aroylhydrazone, $C_6H_4(o\text{-OH})$–CHNNH–$C(O)C_6H_4$–X (X = *p*-H, *p*-OCH_3, *p*-NO_2, *m*-NO_2, *o*-OH), yields the tetrahydrofuran (THF) adduct of $(C_{14}H_9N_2O_2X)_2InC_2H_5$. With formylferrocenyl–aroylhydrazones $C_5H_5FeC_5H_4$–CHNNH–$C(O)C_6H_4$–X (X = *p*-H, *p*-OCH_3, *p*-NO_2, *m*-NO_2, *p*-Cl, *o*-Cl), the diethylindium–hydrazone complex, $(C_{18}H_{14}N_2OFeX)In(C_2H_5)_2$, was formed. With salicylaldehyde–ferrocenoylhydrazone, $C_6H_4(o\text{-OH})$–CHNNH–C-(O)$C_5H_4FeC_5H_5$, the monohydrazone complex $(C_{18}H_{15}N_2O_2Fe)In(C_2H_5)_2$ tetrahydrofuran solvate was obtained. The crystal structures of the *p*-OCH_3 derivatives of the first two series of complexes and of the ferrocenoylhydrazone derivative were determined. In the solid state, the three complexes are dimers, containing a set of seven, three and five fused rings, respectively. In every case, it was observed a symmetric *anti* arrangement of fused rings in relation to a central In_2O_2 four-membered ring, resulting in a configuration that resembles a chair. Cyclic voltammetric studies on the ferrocenylaroylhydrazone complexes revealed electron transference from the ferrocene group towards the indium atom, while for the salicilaldehyde–ferrocenoyl complex this was not observed.

1. Introduction

Trialkylindium compounds, InR_3, react with a variety of substrates containing acidic hydrogen (LH), such as thiols, [1,2] carboxylic acids, [3] amines, [4–6] oximes, [7] and phosphines, [8] via alkane elimination, to produce the corresponding dialkylindium derivatives, R_2InL. When L is an oxygen or a nitrogen ligand, the corresponding R_2InL molecules present intermolecular interactions to produce dimers containing an In_2O_2 or an In_2N_2 four-membered ring.

Aiming to produce new organoindium compounds of general structure R_2InL, we have set out to study the reactions of triethyl indium with hydrazone ligands, including ferrocenyl and ferrocenoylhydrazones. The results lead to hydrazone complexes of indium containing new modes of coordination, which also exhibit molecular interactions leading to dimers containing In_2O_2 four-membered rings.

2. Experimental

2.1. General

Preparation and handling of starting materials and products were conducted under argon atmosphere, using standard Schlenk techniques. Solvents were dried by standard methods and freshly distilled prior to use.

---

* Corresponding author. Tel.: + 55-55-220-8868; fax: + 55-55-220-8031.

E-mail address: peppe@quimica.ufsm.br (C. Peppe).

0022-328X/01/$ - see front matter
PII: S0022-328X(01)00961-5

^{1}H- and ^{13}C-NMR spectra were recorded on a BRUKER AC-P-200 spectrometer with TMS as internal standard. IR spectra were obtained on a Nicolet FTIR 170 SX spectrometer with KBr pellets. Elemental analyses were carried out on a Perkin–Elmer 240 C analyser. Melting points were determined on a PHMK apparatus and are uncorrect. FAB mass spectra of CH_2Cl_2 solutions of **2a**–**e** and **6** were recorded on a VG Autospec double-focusing mass spectrometer operating at 30 kV, xenon was the primary beam gas and nitrobenzylalcohol (NBA) was the matrix; the spectra of **4a**–**f** were recorded on a VG-ZAB-HS spectrometer operating at 8 kV.

2.2. Reagents and ligands

Triethyl indium (Et_3In) was prepared as described by Todt and Dotzer [9]. A Et_2O solution of $InCl_3$ reacted with a twofold excess of a 6 M solution of C_2H_5MgCl in ether. The exothermic reaction leads to a mild reflux of the mixture. After the initial heat evolved has ceased, the mixture is heated under reflux for 3 h with continuous stirring. The ether is distilled and after the removal of the solvent, Et_3In is distilled at 150 °C/10 Torr. For complete removal of the Et_2O, a further distillation through a column is necessary.

Salicylaldehyde–aroylhydrazones, C_6H_4(*o*-OH)–CH-NNH–C(O)C_6H_4–X, **1a**–**e** (see Scheme 1 for structural dependency on X) were prepared by the condensation of salicylaldehyde with the corresponding aroylhydrazine in anhydrous methanol, according to literature procedures [10,11].

Ferrocenyl–aroylhydrazones, $C_5H_5FeC_5H_4$–CH=NNH–C(O)C_6H_4–X, **3a**–**f** (see Scheme 1 for structural dependency on X) were prepared by condensation of ferrocenylaldehyde and the corresponding aroylhydrazine according to the reported methods [12,13].

Salicylaldehyde–ferrocenoylhydrazone, **5**, was prepared by the drop-wise addition of a salicylaldehyde (1.22 g, 1.05 ml, 10 mmol) solution in 50 ml of anhydrous MeOH to a solution of ferrocenoylhydrazine (2.44 g, 10 mmol) in 50 ml of anhydrous MeOH over a period of 10 min with continuous stirring. Then, several drops of glacial AcOH were added and the mixture was taken to reflux for 2 h. The resulting solution was concentrated in vacuum to 10 ml. Addition of Et_2O to the solution lead to the precipitation of an orange-yellow solid, which was recrystallized from $CHCl_3$–petroleum ether (60–90 °C) at −20 °C to give orange crystals (2.85 g, 8.19 mmol, 81.9%). ^{1}H-NMR (DMSO-*d*$_6$, 200 MHz): δ 4.22 (s, 5H, C_5H_5), 4.51 (s, 2H, C_5H_4-β-H), 4.80 (d, 2H, C_5H_4-α-H), 6.97 (q, 2H, C_6H_4),

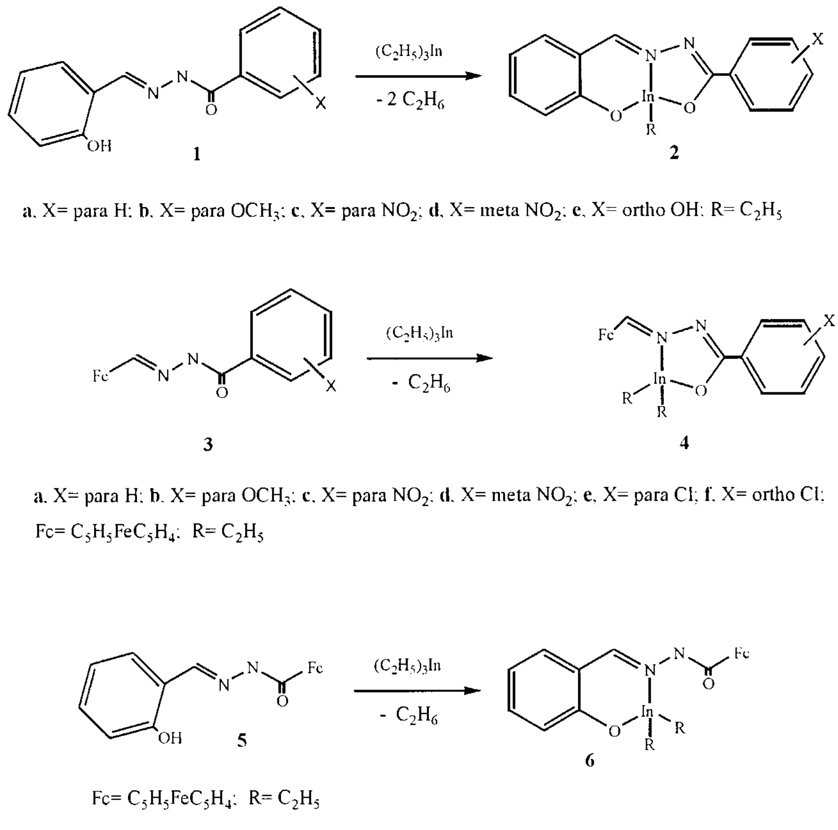

a, X= para H; **b**, X= para OCH_3; **c**, X= para NO_2; **d**, X= meta NO_2; **e**, X= ortho OH; R= C_2H_5

a, X= para H; **b**, X= para OCH_3; **c**, X= para NO_2; **d**, X= meta NO_2; **e**, X= para Cl; **f**, X= ortho Cl;
Fc= $C_5H_5FeC_5H_4$; R= C_2H_5

Fc= $C_5H_5FeC_5H_4$; R= C_2H_5

Scheme 1.

7.37 (m, 1H, C_6H_4), 7.62 (d, 1H, C_6H_4), 8.74 (s, 1H, –CH=N), 11.74 (s, 1H, OH). IR (KBr, cm^{-1}): $\nu_{C=O}$ 1610.6, vs.

2.3. Preparation of hydrazone complexes of indium

2.3.1. Ethyl-(salicylaldehyde–aroylhydrazone)-indium(III), 2

All five compounds, **2a**–**e**, were prepared by the following standard procedure: a solution of Et_3In (125 mg, 0.62 mmol) in 10 ml of toluene was added dropwise to a solution of an equimolar amount of the corresponding salicylaldehyde–aroylhydrazone C_6H_4(*o*-OH)–CHNNH–C(O)C_6H_4–X, **1** in 20 ml of toluene. This mixture was kept under continuous stirring for 30 h at room temperature (r.t.). All the volatiles were removed under vacuum and the residue was recrystallized from a THF–hexane solution to produce yellow crystals of $(C_{18}H_{14}N_2OFeX)In(C_2H_5)_2(THF)$, **2**. Yields: **2a**, 239 mg, 0.26 mmol, 85%; **2b**, 205 mg, 0.21 mmol, 68%; **2c**, 235 mg, 0.24 mmol, 77%; **2d**, 245 mg, 0.25 mmol, 79%; **2e**, 215 mg, 0.23 mmol, 74%.

2.3.2. Diethyl-(ferrocenyl–aroylhydrazone)-indium(III), 4

The six compounds, **4a**–**f**, were prepared by the following standard procedure: to a suspension of 0.62 mmol of the corresponding ferrocenyl–aroylhydrazone $C_5H_5FeC_5H_4$–CHNNH–C(O)C_6H_4–X, **3** in 20 ml of toluene, Et_3In (125 mg, 0.62 mmol) was added. The suspension immediately turned into a brown solution. The reaction mixture was stirred for 24 h at r. t. All the volatiles were removed under vacuum and the residue was recrystallized from a THF–petroleum ether (30–60 °C) mixture to give $(C_{18}H_{14}N_2OFeX)In(C_2H_5)_2$, **4** as red transparent crystals. Yields: **4a**, 219 mg, 0.22 mmol, 71%; **4b**, 262 mg, 0.25 mmol, 81%; **4c**, 272 mg, 0.25 mmol, 81%; **4d**, 248 mg, 0.23 mmol, 74%; **4e**, 274 mg, 0.25 mmol, 81%; **4f**, 274 mg, 0.25 mmol, 81%.

2.3.3. Diethyl-(salicylaldehyde–ferrocenoylhydrazone)-indium(III), 6

A solution of Et_3In (125 mg, 0.62 mmol) in 5 ml of toluene was added to a solution of C_6H_4(*o*-OH)–CHNNH–C(O)$C_5H_4FeC_5H_5$, **5** (212.3 mg, 0.61 mmol) in 15 ml of toluene. After 24 h of continuous stirring at r.t., the reaction solution precipitated a brown–yellow solid. The precipitate was filtered, and recrystallized from THF–hexane to give brown-yellow crystals of $(C_{18}H_{15}N_2O_2Fe)In(C_2H_5)_2$.THF, **6** as a THF adduct (296 mg, 0.25 mmol, 81%).

2.4. Electrochemical measurements

Cyclic voltammograms of **3**–**6** were obtained from a BAS-100 B electrochemical analyzer (Purdue Research Park) equipped with a three-electrode assembly. The solutions were 0.1 mol l^{-1} in CH_2Cl_2 containing *n*-Bu_4NPF_4 as supporting electrolyte. The working electrode was a platinum disk of 1.5 mm in diameter embedded in a cobalt glass seal and it was polished consecutively with polishing alumina and diamond suspensions between runs. The reference electrode was a KCl saturated calomel electrode (SCE). A platinum wire was used as an auxiliary electrode. The solutions were saturated and blanketed with N_2 before the first scan. Measurements were made at r.t. The voltammograms were scanned over the potential range 0–1.0 V (positive potential direction in forward mode), and the scan rates employed were 100 and 200 mV s^{-1}.

2.5. Crystallographic measurements

Crystals of **2b**, **4b** and **6** were mounted in thin-walled glass capillaries and sealed under an argon atmosphere for crystallographic studies (see Table 3 for details). Data were collected on a BRUKER SMART 1000 diffractometer equipped with a graphite monochromator. Data collection was performed with Mo–K_α radiation ($\lambda = 0.71073$ Å) using hemisphere strategy. The structure was solved by direct methods (SHELX-97) and successive difference Fourier maps. The hydrogen atoms were calculated and included as riding atoms in the refinements. The final refinement by full-matrix least-squares methods with anisotropic thermal parameters for non-hydrogen atoms converged to the respective unweighted (*R*1) and weighted (*wR*2) agreement factors. The highest peak on the final difference Fourier map had acceptable heights for all three compounds. All calculations were performed using the SHELXTL program system.

3. Results and discussion

3.1. Preparative and crystallographic studies

We chose to start the synthesis of hydrazone complexes of indium by reacting triethyl indium with a set of five salicylaldehyde–aroylhydrazones C_6H_4(*o*-OH)–CHNNH–C(O)C_6H_4–X, **1** (Scheme 1).

Elimination of two equivalents of ethane leads to the ethyl - (salicylaldehyde–aroylhydrazone) - indium(III) derivatives $(C_{18}H_{14}N_2OFeX)In(C_2H_5)_2(THF)$, **2**. Empirical formulae for **2** were confirmed by C, H and N microanalysis (Table 1) and mass spectrometry (Table 2). The most prominent difference between the infrared spectra of ligands **1** and their corresponding complexes **2** is the disappearance, upon complexation, of the strong carbonyl stretching found at ca. 1610 cm^{-1} in **1**. This is in keeping with the transformation of the carbonyl into an enol functional group as depicted in Scheme 1.

Table 1
Analytical results and melting points (°C) for hydrazone complexes of indium

Compound molecular formula	Melting point (°C)	C (%)		H (%)		N (%)	
		Found	Calc.	Found	Calc.	Found	Calc.
2a $C_{40}H_{46}N_4In_2O_6$	220–221	52.70	52.88	4.79	5.10	6.12	6.17
2b $C_{42}H_{50}N_4In_2O_8$	245–247 [a]	52.01	52.08	5.18	5.20	5.85	5.78
2c $C_{40}H_{44}N_6In_2O_{10}$	254–255 [a]	48.40	48.12	4.23	4.44	8.97	8.41
2d $C_{40}H_{44}N_6In_2O_{10}$	>250	48.05	48.12	4.40	4.44	8.12	8.41
2e $C_{40}H_{46}N_4In_2O_8$	238–240 [a]	50.89	51.09	4.85	4.93	6.18	5.95
4a $C_{44}H_{50}Fe_2In_2N_4O_2$	157–158	52.18	52.42	4.93	5.00	5.61	5.55
4b $C_{46}H_{54}Fe_2In_2N_4O_4$	158–160	51.69	51.72	5.09	5.10	5.22	5.24
4c $C_{44}H_{48}Fe_2In_2N_6O_6$	145–147	48.13	48.12	4.37	4.41	7.52	7.65
4d $C_{44}H_{48}Fe_2In_2N_6O_6$	174–176	47.99	48.12	4.39	4.41	7.69	7.65
4e $C_{44}H_{48}Fe_2In_2N_4O_2Cl_2$	145–147	48.94	49.06	4.25	4.49	5.15	5.20
4f $C_{44}H_{48}Fe_2In_2N_4O_2Cl_2$	187–189	49.08	49.06	4.50	4.49	5.25	5.20
6 $C_{52}H_{66}Fe_2In_2N_4O_6$	142–144	52.87	52.73	5.22	5.62	5.05	4.73

[a] With decomposition.

Table 2
Important mass spectra data for hydrazone complexes of indium [a]

Compound	$[DH]^+$	[D]+	$[D–THF]^+$	$[DH–2THF]^+$	$[MH]^+$	$[MH–THF]^+$	$[M–C_2H_5]^+$	**3**	$[(C_2H_5)_2In]^+$
2a	–	–	–	765(9)	–	383(100)	–	–	–
2b	969(1.5)	968(6)	896(5)	–	–	413(6)	–	–	–
2c	999(6)	998(4)	926(3)	–	–	428(15)	–	–	–
2d	–	–	–	–	–	428(15)	–	–	–
2e	–	–	–	–	–	399(12)	–	–	–
4a	–	–	–	–	505(43)	–	475(53)	332(40)	173(63)
4b	–	–	–	–	535(19)	–	505(13)	362(22)	173(59)
4c	–	–	–	–	550(8)	–	520(14)	377(6)	173(29)
4d	–	–	–	–	550(16)	–	520(22)	377(8)	173(38)
4e	–	–	–	–	539(19)	–	509(21)	366(22)	173(33)
4f	–	–	–	–	539(8)	–	509(1)	366(26)	173(13)
6	1185(3)	1184(2)	–	1041(2)	–	521(22)	–	–	–

[a] D, dimeric species; M, monomeric species; THF, tetrahydrofuran ligand.

The structure of **2b** was solved by X-ray diffraction techniques. Details of crystal data, intensity collection and structural refinement are given in Table 3. The structure of the molecule is shown in Fig. 1; and bond distance and angles in Table 4.

The compound, in the solid state, is a dimer containing two molecules of the recrystallizing solvent, THF, coordinated to each of the metal centers. The dimerization occurs through the carbonyl oxygen atom of the aroylhydrazone. The structure is centrosymmetric with hexa-coordinated indium atoms. The resulting dimer contains a set of seven fused rings, including two In–N–N–C–O five-membered, two In–N–C–C–C–O sixmembered, two aromatic C_6H_4, and one In_2O_2 four-membered heterocycles. The hydrazone ligands assume an *anti*-configuration to the planar In_2O_2 ring, resembling a chair, in which the four-membered In_2O_2 ring is the seat and the two hydrazone ligands are at opposite edges almost perpendicular to the In_2O_2 ring. The THF molecule and the ethyl group complete the hexa-coordination sphere around each metal center by occupying the free space in the front and in the back of the chair (THF) and at the top and the bottom (C_2H_5). The methyl group of the ethyl ligand, C(16), is disordered and this has been considered in the calculations by refining two positions for C(16) with half occupancy per position.

The In–O bond lengths in the In_2O_2 ring with tri-coordinated oxygen atoms are not identical with In(1)–O(1) being 2.199(2) Å while In(1)–O(1A) is 2.243(2) Å. The other In–O bonds, namely In(1)–O(2) and In(1)–O(3) measure 2.172(2) and 2.517(3) Å, respectively. The distances of first three In–O bonds are in the range of 2.10–2.20 Å, normally observed for other indium complexes containing four-membered In_2O_2 rings derived of alcoxydes, [14,15] salen type ligands [16], and phenoxydes [17], in which secondary bonds can measure up to the value of 2.38 Å as observed for dimethyl-(salicylaldehyde)-indium(III) [17]. A considerably longer In–O distance is observed

Table 3
Crystal data and structural refinement parameters for the hydrozone complexes of indium

Compound	**2b**	**4b**	**6**
Empirical formula	$C_{42}H_{50}In_2N_4O_8$	$C_{46}H_{54}Fe_2In_2N_4O_4$	$C_{52}H_{66}Fe_2In_2N_4O_6$
Formula weight	968.50	1068.27	1184.43
Crystal dimensions (mm)	0.20 × 0.25 × 0.30	0.10 × 0.20 × 0.25	0.20 × 0.25 × 0.30
Crystal system	Triclinic	Monoclinic	Monoclinic
Space group	$P\bar{1}$	$P2_1/c$	$P2_1/n$
Unit cell dimensions			
a (Å)	8.3985(12)	12.9278(9)	9.9815(10)
b (Å)	10.7828(15)	14.2991(9)	14.8792(15)
c (Å)	12.4425(17)	12.6469(9)	17.8916(17)
α (°)	96.775(3)	90	90
β (°)	99.946(3)	110.664(1)	91.333(2)
γ (°)	106.463(2)	90	90
V (Å^3)	1047.6(3)	2187.4(3)	2656.5(5)
Z	1	2	2
D_{calc} (g cm^{-3})	1.535	1.622	1.481
Absorption coefficient (mm^{-1})	1.156	1.738	1.422
Temperature (K)	298 (2)	293 (2)	298 (2)
Theta range for data collection (°)	1.69–25.03	1.68–25.02	1.78–25.03
Reflections collected	4369	8973	10 905
Reflections observed [$I>2\sigma(I)$]	3671	3864	4691
Number of parameters	252	262	298
R_1	0.031	0.029	0.039
wR_2	0.076	0.066	0.088
Largest difference peak and hole (e Å^{-3})	0.522 and −0.367	0.651 and −0.384	0.481 and −0.524

for the indium–THF bond, In(1)–O(3)=2.517(3) Å; but again is in the range of 2.33–2.58 Å in a series of THF adducts of penta-coordinated organoindium compounds synthesized by Gabbai and co-workers [18–21]. The In(1)–N(1) bond distance of 2.231(3) Å is very similar to the values of 2.25–2.26 Å reported for compounds containing salen types of ligands with imine binding sites [16,22]. The last bond on the octahedral sphere of coordination around the indium, the In(1)–C(15) = 2.130 Å, is in the range of 2.11–2.21 Å reported in the literature [14,15,18–23]. The N(1)–N(2), N(2)–C(8) and C(8)–O(2) distances observed in the =N–N=C(O$^-$)- fragment of the ligand in the complex **2b** are 1.386(4), 1.312(4) and 1.286(4) Å, respectively; these distances are consistent with the enolate form of the amide functionality in the complexes [24–26], binding the indium center through the phenolate-O, imine-N, and deprotonated amide-O atoms.

A set of six ferrocenyl–aroylhydrazones $C_5H_5FeC_5H_4$–CHNNH–C(O)C_6H_4-X, **3** (Scheme 1) react with trietylindium to produce a set of new organoindium ferrocenyl-hydrazone derivatives ($C_{18}H_{14}N_2OFeX$)In(C_2H_5)$_2$, **4**. Empirical formulae **4** were confirmed by C, H and N microanalysis (Table 1) and mass spectrometry (Table 2). The infrared spectra of complexes **4**, suggest deprotonation of NH groups of the hydrazones and transformation of the carbonyl into an enol functional group, as observed for **2**. The structure of **4b** was determined by X-ray diffraction. Details of crystal data, intensity collection and structural refinement are given in Table 3. The structure of the molecule is shown in Fig. 2; and bond distances and angles in Table 5. The structure of the complex is very similar to that of **2b**; however, a few structural differences merit comment. This dimer contains a set of three fused rings, including two $\overline{\text{In–N–N–C–O}}$ five-membered and one In_2O_2 four-membered heterocycles, with *anti* hydrazone ligands relative to the planar In_2O_2 ring. The geometry around the indium atoms is a highly distorted square pyramid, an unusual structure for penta-coordinated indium

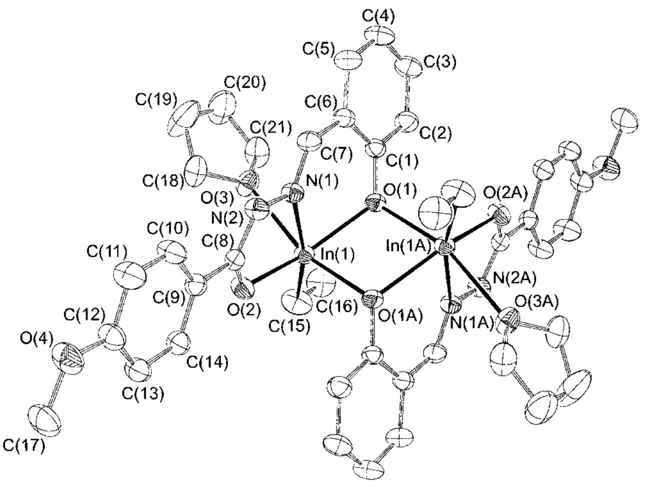

Fig. 1. The molecular structure of $C_{42}H_{50}In_2N_4O_8$, **2b**, (ORTEP diagram), with atoms shown as 30% probability ellipsoids. Hydrogen atoms have been omitted for clarity.

Table 4
Selected bond lengths (Å) and bond angles (°) for **2b** [a]

Bond lengths					
In(1)–O(1)	2.199(2)	O(1)–In(1A)	2.243(2)	C(15)–C(16′)	1.33(1)
In(1)–O(1A)	2.243(2)	O(1)–C(1)	1.351(4)	C(16)–C(16′)	1.63(1)
In(1)–O(2)	2.172(2)	O(2)–C(8)	1.286(4)	C(6)–C(7)	1.422(5)
In(1)–O(3)	2.517(3)	N(1)–N(2)	1.386(4)	C(8)–N(2)	1.312(4)
In(1)–N(1)	2.231(3)	N(1)–C(7)	1.289(4)	C(8)–C(9)	1.461(5)
In(1)–C(15)	2.130(3)	C(15)–C(16)	1.43(1)		
Bond angles					
O(1)–In(1)–O(1A)	75.08(2)	In(1)–O(1)–C(1)	125.0(2)		
O(1)–In(1)–O(2)	146.7(1)	In(1A)–O(1)–C(1)	117.1(2)		
O(1)–In(1)–O(3)	89.76(9)	In(1)–O(2)–C(8)	114.8(2)		
O(1)–In(1)–N(1)	78.9(1)	In(1)–O(3)–C(18)	120.0(3)		
O(1)–In(1)–C(15)	108.0(1)	In(1)–O(3)–C(21)	131.4(3)		
O(1A)–In(1)–O(2)	91.39(9)	In(1)–N(1)–N(2)	116.2(2)		
O(1A)–In(1)–O(3)	163.30(9)	In(1)–N(1)–C(7)	127.3(2)		
O(1A)–In(1)–N(1)	93.0(1)	N(2)–N(1)–C(7)	116.1(3)		
O(1A)–In(1)–C(15)	100.2(2)	In(1)–C(15)–C(16)	116.5(6)		
O(2)–In(1)–O(3)	97.85(9)	In(1)–C(15)–C(16′)	126.5(5)		
O(2)–In(1)–N(1)	71.53(9)	N(1)–C(7)–C(6)	125.6(3)		
O(2)–In(1)–C(15)	104.2(1)	N(1)–N(2)–C(8)	111.2(3)		
O(3)–In(1)–N(1)	76.9(1)	O(2)–C(8)–N(2)	125.5(3)		
O(3)–In(1)–C(15)	91.0(2)	O(2)–C(8)–C(9)	117.6(3)		
N(1)–In(1)–C(15)	166.3(2)	N(2)–C(8)–C(9)	116.9(3)		
In(1)–O(1)–In(1A)	104.92(9)				

[a] Symmetry equivalent position is $-x+2$, $-y$, $-z+2$.

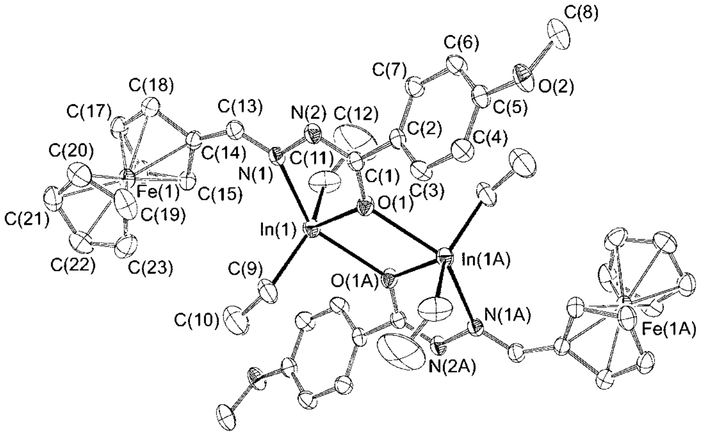

Fig. 2. The molecular structure of $C_{46}H_{54}Fe_2In_2N_4O_4$, **4b**, (ORTEP diagram), with atoms shown as 30% probability ellipsoids. Hydrogen atoms have been omitted for clarity.

compounds, which preferentially assume trigonal-bipyramidal geometry [7,27–29]. The N(1)O(1A)In(1)C(9)C(11) skeleton forms the square base, containing the N(1)–O(1A) and C(9)–C(11) pairs of atoms in a *trans* position. The oxygen atom O(1) assumes the apical position in the geometrical arrangement. The bond angles O(1)–In(1)–O(1A) [71.98 (9)°] and O(1)–In(1)–N(1) [69.63 (9)°] are both considerably smaller than 90°, while the pair of angles O(1)–In(1)–C(9) [104.8 (1)°] and O(1)–In(1)–C(11) [108.9 (2)°] are greater than the required 90° for a regular base; thus, the distortion can be understood as the O(1A)–In(1)–N(1) diagonal is tilted towards the apical O(1) atom, while the second diagonal, C(9)–In(1)–C(11) is tilted away from the apical O(1) atom. Comparison of the interatomic distances involving the indium atom between compounds **4b** and **2b** reveals some significant differences. We shall start discussing the In–O bond lengths of the In_2O_2 four-membered ring. The primary In(1)–O(1) bonds in both cases (**2b** = 2.199(2) Å; **4b** = 2.205(2) Å) have the same length, within the experimental error; while the secondary bond in **4b**, In(1)–O(1A) = 2.482(2) Å is longer than the corresponding bond in **2b**, In(1)–O(1A) = 2.243(2) Å. The reason for such a difference is a considerable steric hindrance between the ethyl group [C(9)–C(10)] from one of the molecules of the dimer **4b** and the phenyl group [C(2A)–C(7A)] of the methoxy-aroyl portion of the hydrazone ligand of the second molecule of the dimer **4b**. This same argument is also responsible for compression [O(1)–In(1)–O(1A) = 71.98(9)°] and expansion [In(1)–O(1)–In(1A) = 108.02(9)°] of the angles in the In_2O_2 ring in **4b** when compared with the analogous [O(1)–In(1)–O(1A) = 75.08(2)°] and [In(1)–O(1)–In-(1A) = 104.92(9)°] angles in **2b**. The final significant difference between the two compounds is the In(1)–N(1) bond length, related to the interaction of the metal with the imine binding site of the hydrazone ligands. The observed distance in **4b** [2.411(3) Å] is longer than the measured value in **2b** [2.231(3) Å]; the reasons that lead one to understand such a difference are the following: in **2b**, the imine binding site is attached to an *ortho* position of a phenoxide ligand, which also is coordinated to the metal center leading to a rigid and planar tridentate chelate mode of coordination; while in **4b** the imine binding site is attached to a bulky ferrocenyl group, which develops repulsive interactions particularly with the ethyl group [C(9)–C(10)] located at *cis* position to the imine nitrogen ligand. The bond lengths C(1)–O(1) [1.317(4) Å] and C(1)–N(2) [1.292(4) Å], are again consistent with an enolized form of the ligand to give an O–C=N–N=C–R conjugated system [24,30].

A third type of related ligand is salicylaldehyde–ferrocenoylhydrazone $C_6H_4(o\text{-OH})\text{–CHNNH–C(O)}C_5H_4\text{-}FeC_5H_5$, **5**. The reaction between **5** and triethylindium gives the complex $(C_{18}H_{15}N_2O_2Fe)In(C_2H_5)_2$, **6** containing one THF molecule held loosely in the lattice. Adduct formation, in this case, follows a different pathway (Scheme 1) than verified for ligands **1** and **3**. The observed product results from the elimination of only one equivalent of ethane, and we have not observed enolization of the carbonyl group of the hydrazone ligand as revealed by the strong carbonyl stretching vibration in the infrared spectrum of **6** at 1613.3 cm^{-1}, readily comparable to the carbonyl stretching in the free ligand, observed at 1610.6 cm^{-1}. As revealed by the crystal structural determination (see Table 3 for details of crystal data, intensity collection and structural refinement, Fig. 3 for molecular structure; and Table 6 for bond distance and angles), coordination of the hydrazone ligand to the metal center follows a bidentade fashion involving the imine nitrogen and the phenolic-oxygen groups of the ligand as binding sites, giving rise to a centrosymetric dimer held together by secondary interactions between the phenolic oxygens and the indium atoms, each from the different units that compose the dimer.

Compound **6** contains a set of five fused rings with two six-membered $\overline{\mathrm{In{-}O{-}C{-}C{-}C{-}N}}$ heterocycles, *anti* to each other, fused to a central In_2O_2 four-membered ring. This arrangement is again similar to the chair described for compound **2b**. The geometry around the indium metal is a highly distorted square pyramid, similar to compound **4b**; here the square base is formed by the C(19)C(21)In(1)O(1A)N(2) atoms, in which the carbon atoms are *trans* to each other and the diagonal C(19)–In(1)–C(21) tilted away from the O(1) apical atom, while the diagonal O(1A)–In(1)–N(2) is tilted towards to the apical substituent. The bonding distances within the coordination sphere of indium in **6** are all similar to the values measured in **4b**; thus the differences between these parameters and the parameters for **2b** can all be understood by similar arguments to the already used above when were discussed the features of structure **4b**.

Table 5
Selected bond lengths (Å) and bond angles (°) for **4b** [a]

Bond lengths					
In(1)–O(1)	2.205(2)	O(1)–In(1A)	2.482(2)	C(9)–C(10)	1.482(6)
In(1)–O(1A)	2.482(2)	O(1)–C(1)	1.317(4)	C(11)–C(12)	1.372(9)
In(1)–N(1)	2.411(3)	N(1)–N(2)	1.418(4)	N(2)–C(1)	1.292(4)
In(1)–C(9)	2.158(4)	N(1)–C(13)	1.284(4)	C(1)–C(2)	1.499(4)
In(1)–C(11)	2.154(5)				
Bond angles					
O(1)–In(1)–O(1A)	71.98(9)	In(1)–O(1)–C(1)	116.8(2)		
O(1)–In(1)–N(1)	69.63(9)	In(1A)–O(1)–C(1)	132.5(2)		
O(1)–In(1)–C(9)	104.8(1)	In(1)–N(1)–N(2)	112.8(2)		
O(1)–In(1)–C(11)	108.8(2)	In(1)–N(1)–C(13)	135.3(2)		
O(1A)–In(1)–N(1)	141.08(8)	N(2)–N(1)–C(13)	111.8(3)		
O(1A)–In(1)–C(9)	94.1(1)	In(1)–C(9)–C(10)	119.5(4)		
O(1A)–In(1)–C(11)	95.5(2)	In(1)–C(11)–C(12)	118.7(5)		
N(1)–In(1)–C(9)	101.6(1)	N(1)–N(2)–C(1)	112.6(3)		
N(1)–In(1)–C(11)	90.8(2)	O(1)–C(1)–N(2)	126.9(3)		
C(9)–In(1)–C(11)	146.3(2)	O(1)–C(1)–C(2)	117.6(3)		
In(1)–O(1)–In(1A)	108.02(9)	N(2)–C(1)–C(2)	115.5(3)		

[a] Symmetry equivalent position is $-x+1$, $-y$, $-z$.

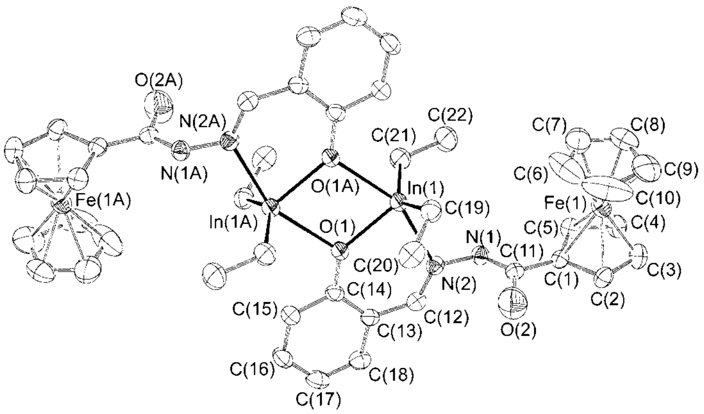

Fig. 3. The molecular structure of $C_{52}H_{66}Fe_2In_2N_4O_6$, **6**, (ORTEP diagram), with atoms shown as 30% probability ellipsoids. Hydrogen atoms have been omitted for clarity.

Table 6
Selected bond lengths (Å) and bond angles (°) for **6** [a]

Bond lengths					
In(1)–O(1)	2.179(3)	O(1)–In(1A)	2.488(3)	C(21)–C(22)	1.522(7)
In(1)–O(1A)	2.488(3)	O(1)–C(14)	1.330(5)	N(1)–C(11)	1.266(5)
In(1)–N(2)	2.375(4)	N(2)–N(1)	1.409(5)	C(11)–O(2)	1.519(6)
In(1)–C(19)	2.143(5)	N(2)–C(12)	1.271(5)	C(11)–C(1)	1.453(6)
In(1)–C(21)	2.155(5)	C(19)–C(20)	1.515(7)	C(12)–C(13)	1.450(6)
Bond angles					
O(1)–In(1)–O(1A)	75.7(1)	In(1A)–O(1)–C(14)	121.0(3)		
O(1)–In(1)–N(2)	79.7(1)	In(1)–N(2)–N(1)	113.6(3)		
O(1)–In(1)–C(19)	107.0(2)	In(1)–N(2)–C(12)	128.1(3)		
O(1)–In(1)–C(21)	110.2(2)	N(1)–N(2)–C(12)	116.8(4)		
O(1A)–In(1)–N(2)	155.4(1)	In(1)–C(19)–C(20)	114.7(4)		
O(1A)–In(1)–C(19)	90.7(1)	In(1)–C(21)–C(22)	116.4(4)		
O(1A)–In(1)–C(21)	93.2(1)	N(2)–N(1)–C(11)	119.0(4)		
N(2)–In(1)–C(19)	97.1(2)	N(1)–C(11)–O(2)	124.8(4)		
N(2)–In(1)–C(21)	94.7(2)	N(1)–C(11)–C(1)	117.1(4)		
C(19)–In(1)–C(21)	142.3(2)	O(2)–C(11)–C(1)	118.1(4)		
In(1)–O(1)–In(1A)	104.3(1)	N(2)–C(12)–C(13)	126.4(4)		
In(1)–O(1)–C(14)	134.6(3)	O(1)–C(14)–C(13)	124.5(4)		

[a] Symmetry equivalent position is $-x, -y+1, -z+1$.

3.2. Spectroscopic results

Tables 7 and 8 show the ^{1}H- and ^{13}C-NMR spectra of the compounds prepared in this work. We first note at the ^{1}H spectra that the resonance signals of the OH and/or NH groups in the free ligands **1** and **3**, observed between 10–12 ppm, disappear upon complexation leading to **2** and **4**. On the contrary, the N–H singlet observed at 11.74 ppm for ligand **5** is kept upon complexation leading to **6** at 12.10 ppm. Integration measurements at the ^{1}H spectra confirm the molar ratio ethyl groups:hydrazone ligand of 1:1 for compound **2** and 2:1 for **4** and **6**. In the solid state, the dimers have no mirror plane of symmetry thus the methylne protons of the ethyl groups are diastereotopic. The absence of the characteristic pattern of diastereotopic protons in the ^{1}H-NMR suggests the formation of monomers in solution, as also indicated by the electrochemical studies (see below).

3.3. Electrochemical results

The cyclic voltammetric data of ferrocene, ferrocene-containing ligands **3a**–**f** and **5** and their indium complexes **4a**–**f** and **6** are given in Table 9. The focus of our attention was on the Fe^{II}/Fe^{III} oxidation processes in the free ligands and their complexes. The parameters of interest are the anodic (E_{pa}), cathodic (E_{pc}), formal reduction potentials $E^{\circ\prime} = 1/2(E_{pa} + E_{pc})$ [31], and the corresponding anodic (i_{pa}) and cathodic (i_{pc}) peak currents and their ratios (i_{pc}/i_{pa}). The corresponding data for ferrocene is also displayed in Table 9 for comparison.

Table 7
^{1}H-NMR for hydrazone complexes of indium [a]

	2a	**2b**	**2c**	**2d**	**2e**	**4a**	**4b**	**4c**	**4d**	**4e**	**4f**	**6**
InCH_2CH$_3$	0.64(q,2)	0.61(q,2)	0.68(q, 2)	0.69(q, 2)	0.69(q, 2)	0.89(q, 4)	0.85(q, 4)	0.89(s, 4)	0.87(q, 4)	0.87(q, 4)	0.90(q, 4)	0.86(q, 4)
InCH$_2$$CH_3$	1.30(t, 3)	1.28(t, 3)	1.30(t, 3)	1.30(t, 3)	1.30(t, 3)	1.18(t, 6)	1.18(t, 6)	1.18(s, 6)	1.23(t, 6)	1.19(t, 6)	1.22(t, 6)	1.24(t, 6)
C_5H_5	–	–	–	–	–	4.36(s, 5)	4.28(s, 5)	4.33(s, 5)	4.39(s, 5)	4.32(s, 5)	4.32(s, 5)	4.19(s, 5)
H(α)						4.73(s,2)		4.60(s,2)		4.57(s,2)		4.76(s,2)
C_5H_4	–	–	–	–	–		4.52(s,4)		4.62(s,4)		4.58(m,4)	
H(β)	–	–	–	–	–	4.61(s,2)		4.52(s,2)		4.32(s,2)		4.45(s,2)
$C_6H_4X+C_6H_4$ (*ortho* O)	6.48(d,1) 6.64(t,1) 7.12(t,1) 7.24(d,1) 7.39(d,3) 8.05(m,2)	6.43–7.06 (m,4) 7.23–8.02 (dd,4)	6.50–7.24 (m,4) 8.26(m,4)	6.47–7.10 (m,4) 7.29–8.80 (m,4)	6.50–7.89 (m,8)	7.53–8.21 (m,5)	6.91(d,2) 8.00(d,2)	8.24(m,4)	7.60(s,1) 8.27(d,1) 8.46(d,1) 8.80(s,1)	7.38(d,2) 8.05(d,2)	7.61(s,4)	6.83–7.02 (m,2) 7.30(d,2)
CH=N	8.55(s,1)	8.56(s,1)	8.61(s,1)	8.63(s,1)	8.55(s,1)	8.90(s,1)	8.70(s,1)	8.70(s,1)	8.93(s,1)	8.80(s,1)	8.7(s,1)	8.60(s,1)
NH	–	–	–	–	–	–	–	–	–	–	–	12.10(s,1)
THF	1.76(m,4) 3.60(m.4)	1.83(m,4) 3.71(m,4)	1.83(m,4) 3.77(m,4)	1.71(m,4) 3.60(m,4)	1.70(m,4) 3.60(m,4)	–	–	–	–	–	–	1.84(s,4) 3.74(s,4)
OCH_3	–	3.55 (s,3)	–	–	–	–	3.83(s,3)	–	–	–	–	–
OH	–	–	–	–	11.20(s,1)	–	–	–	–	–	–	–

[a] **2a**–**e** (in DMSO-d_6); **4a**–**f** and **6** (in $CDCl_3$); in ppm from Me_4Si; s, singlet; d, doublet; dd, doublet of doublets; t, triplet; q, quartet; m, multiplet; numbers in parentheses correspond to relative integration.

Table 8
^{13}C-NMR for hydrazone complexes of indium [a]

	2a	**2b**	**2c**	**2d**	**2e**	**4a**	**4b**	**4c**	**4d**	**4e**	**4f**	**6**
InCH_2CH$_3$	7.79	8.00	7.91	7.85	7.84	10.73	9.31	9.28	10.73	10.82	10.73	10.26
InCH$_2$$CH_3$	11.87	11.86	11.92	11.82	11.70	11.15	11.16	11.10	11.08	11.16	11.18	11.56
C_5H_5	–	–	–	–	–	69.72	69.69	69.84	69.82	69.78	69.77	69.48
C(α)				67.00	67.10	71.99	71.82	72.39	72.52	72.25	72.10	70.63
C_5H_4	–	–	–	–								
C(β)				25.12	25.13	68.16	67.97	68.23	68.15	68.33	68.65	67.78
$C_6H_4X+C_6H_4$ (*ortho* O)	113.39	113.15	113.70	113.58	113.65	122.82	113.40	123.18	122.81	123.91	122.82	115.98
	118.90	119.03	118.69	118.67	116.25	127.79	128.12	128.83	124.80	128.33	126.67	118.78
	121.84	121.77	122.10	121.39	118.06	128.16	129.49	141.90	128.85	129.26	130.00	122.01
	127.12	128.73	123.30	121.96	118.42	130.27	156.19	158.78	133.45	136.57	130.29	132.20
	127.82	131.50	128.25	124.26	121.39				137.35		139.47	133.62
	129.67	133.79	132.40	129.67	121.91				148.24		146.28	134.67
	131.73	155.57	142.36	132.20	128.67							
	133.96	160.66	148.19	133.22	131.66							
	136.55		148.88	134.23	134.16							
	156.36		158.03	138.35	132.32							
				147.78	156.62							
				157.68	159.06							
CH=N	167.36	167.06	165.03	165.04	157.06	157.30	161.36	160.30	159.95	158.29	159.57	158.09
O–C=N	169.23	169.08	169.60	169.42	169.23	168.68	170.09	167.94	167.86	167.93	167.87	167.20
C(α)	67.10	66.36	67.00		67.00							68.16
THF						–	–	–	–	–	–	
C(β)	25.13	25.14	25.12		25.12							25.72
OCH_3	–	55.13	–	–	–	–	55.29	–	–	–	–	–

[a] **2a**–**e** (in DMSO-d_6); **4a**–**f** and **6** (in $CDCl_3$); in ppm from Me_4Si.

Table 9
Electrochemical data for ferrocenylhydrazone complexes of indium

Compound	V (mV s^{-1})	E_{pa} (mV)	E_{pc} (mV)	$E^{\circ\prime}$ (mV)	i_{pa} ($\times 10^{-7}$ A)	i_{pc} ($\times 10^{-7}$ A)	i_{pc}/i_{pa}
Ferrocene	100	487	396	441.5	20.92	22.59	1.08
	200	494	390	442	28.07	30.32	1.08
3a	100	574	476	525	4.63	3.77	0.81
	200	576	477	526	6.14	5.32	0.87
4a	200	754	516	635	16.78	6.12	0.36
3b	100	562	475	518	9.30	6.75	0.73
	200	560	469	515	11.25	10.29	0.92
4b	100	742	477	610	3.05	3.69	1.21
	200	746	481	614	6.47	6.32	0.98
3c	100	570	482	526	13.12	12.42	0.95
	200	576	482	529	17.13	16.08	0.94
4c	200	750	547	649	14.46	7.72	0.53
3d	100	560	466	513	4.53	4.34	0.96
	200	559	467	513	3.80	3.13	0.82
4d	200	739	513	626	13.17	0.34	0.03
3e	100	549	460	504	16.26	17.66	1.09
	200	552	454	503	21.48	23.67	1.10
4e	200	763	522	642	21.17	11.28	0.53
3f	100	599	497	548	21.22	19.69	0.93
	200	588	508	548	7.98	7.17	0.90
4f	200	729	471	600	8.59	0.44	0.05
5	100	602	523	562.5	8.77	8.38	0.96
	200	601	519	560	11.41	11.41	1
6	100	588	495	541.5	57.13	47.61	0.83
	200	597	500	543.5	13.40	8.92	0.67

All the ligands **3a**–**f** and **5** undergo one-electron reversible redox reactions, as suggested by the i_{pc}/i_{pa} ratio approaching to unity. Furthermore, the observed $E^{\circ\prime}$ values are anodically shifted with respect to that of ferrocene and this shift results from the electron-withdrawing effect of the hydrazone group, which naturally increase the difficulties on their oxidation.

The complexes, which are dimers in the solid state, also exhibit one pair of a Fe^{II}/Fe^{III} redox peak, indicating that the two ferrocenyl groups of the dimers are electrochemically equivalent or that there is a presence of monomeric species in solution. However, except for **4b**, their i_{pc}/i_{pa} ratios are considerably smaller than unity, characterising irreversible redox processes. The observed $E^{\circ\prime}$values for the complexes **4a**–**f** are in the range of 60–120 mV higher than their corresponding ligands **3a**–**f**. This fact suggests electron transference from the ferrocenyl group to the indium atom through π-conjugation involving the cyclopentadienyl ring and the –C=N–N=C– group, and this leads to a decrease in the electron density of ferrocene. On the other hand, when one compares the $E^{\circ\prime}$ potential of complex **6** to its respective ligand **5**, a slight shift of ca. 20 mV towards cathodic potential was observed. Here, there seems to be no significant electron transfer from the ferrocene group towards the indium center.

4. Supplementary material

Crystallographic data for the structural analysis (excluding structure factors) have been deposited with the Cambridge Crystallographic Data Centre, CCDC no. 157200, 157201 and 157202 for compounds **2b**, **6** and **4b**, respectively. Copies of this information may be obtained free of charge from The Director, CCDC, 12 Union Road, Cambridge CB2 1EZ, UK (Fax: +44-1223-336033; e-mail: deposit@ccdc.cam.ac.uk or www: http://www.ccdc.cam.ac.uk).

Acknowledgements

This work was supported by Operating Grants (to C.P.) from CAPES (Brazil) and from the National Natural Science Foundation of China (Grant no. 29872018 to Y.F.Y. and 29972026 to J.T.W.).

References

[1] A.F. Berniaz, D.G. Tuck, J. Organomet. Chem. 46 (1972) 243.

[2] B. Yearwood, S. Ul Ghazi, M.J. Heeg, N. Richardson, J.P. Oliver, Organometallics 19 (2000) 865.

[3] F.W. Einstein, M.M. Gilbert, D.G. Tuck, J. Chem. Soc. Dalton Trans. (1973) 248.

[4] K. Mertz, W. Schwarz, B. Eberwein, J. Weidlein, H. Hess, H.D. Hausen, Z. Anorg. Allg. Chem. 419 (1977) 99.

[5] K.A. Aitchison, J.D.J. Backerdirks, D.C. Bradley, M.M. Faktor, D.M. Frigo, M.B. Hursthouse, B. Hussain, R.L. Short, J. Organomet. Chem. 366 (1989) 11.

[6] G. Rossetto, D. Ajo, N. Brianese, U. Casellato, F. Ossola, M. Porchia, A. Vittadini, P. Zanella, R. Graziani, Inorg. Chim. Acta. 170 (1990) 95–101.

[7] H.M.M. Shearer, J. Twiss, K. Wade, J. Organomet. Chem. 184 (1980) 309.

[8] J.A. Burns, M.D.B. Dillingham, J.B. Hill, K.D. Gripper, W.T. Pennington, G.H. Robinson, Organometallics 13 (1994) 1514.

[9] E. Todt, R. Dotzer, Z. Anorg. Allg. Chem. 321 (1963) 120.

[10] D.K. Rastogi, S.K. Dua, V.B. Rana, S.K. Sahni, J. Inorg. Nucl. Chem. 40 (1978) 1323.

[11] J.D. Ranford, J.J. Vittal, Y.M. Wang, Inorg. Chem. 37 (1998) 1226.

[12] Y.F. Yuan, L.Y. Zhang, A.G. Hu, J.T. Wang, W.Y. Liu, T.Z. Ding, Polyhedron 18 (1999) 1247.

[13] Y.F. Yuan, L.Y. Zhang, W.Q. Qian, J.T. Wang, Transition Met. Chem. 23 (1998) 21.

[14] M. Veith, S. Hill, V. Huch, Eur. J. Inorg. Chem. (1999) 1343.

[15] W. Uhl, S.U. Keimling, S. Pohl, W. Saak, R. Wartchow, Chem. Ber./Recueil. 130 (1997) 1269.

[16] D.A. Atwood, J.A. Jegier, D. Rutherford, Bull. Chem. Soc. Jpn. 70 (1997) 2093.

[17] N.W. Alcock, I.A. Degnan, S.M. Roe, M.G.H. Wallbridge, J. Organomet. Chem. 414 (1991) 285.

[18] M. Tschinkl, A. Schier, J. Riede, F.P. Gabbai, Inorg. Chem. 37 (1998) 5097.

[19] F.P. Gabbai, A. Schier, J. Riede, Angew. Chem. Int. Ed. Engl. 37 (1998) 622.

[20] F.P. Gabbai, A. Schier, J. Riede, A. Sladek, H.W. Görlitzer, Inorg. Chem. 36 (1997) 5694.

[21] M. Tschinkl, A. Schier, J. Riede, E. Schmidt, F.P. Gabbai, Organometallics 16 (1997) 4759.

[22] Y.Z. Shen, Y. Pan, L.Y. Wang, G. Dong, X.P. Jin, X.Y. Huang, H. Hu, J. Organomet. Chem. 590 (1999) 242.

[23] M.A. Khan, C. Peppe, D.G. Tuck, J. Organomet. Chem. 280 (1985) 17.

[24] N.R. Sangeetha, S. Pal, Bull. Chem. Soc. Jpn. 73 (2000) 357 (and references therein).

[25] S.P. Rath, S. Mondal, A. Chakravorty, Inorg. Chim. Acta 263 (1997) 247.

[26] N.R. Sangeetha, C.K. Pal, P. Ghosh, S. Pal, J. Chem. Soc. Dalton Trans. (1996) 3293.

[27] M.A. Khan, R.C. Steevensz, D.G. Tuck, J.G. Noltes, P.W.R. Corfield, Inorg. Chem. 19 (1980) 3407.

[28] J.T. Leman, H.A. Roman, A.R. Barron, Organometallics 12 (1993) 2986.

[29] Y. Zhou, D.S. Richeson, Inorg. Chem. 35 (1996) 2448.

[30] J.T. Wang, F.Q. Liu, Y.W. Zhang, R.J. Wang, H.G. Wang, X.K. Yao, J. Organomet. Chem. 375 (1989) 173.

[31] P.T. Kissinger, W.R. Heineman, J. Chem. Ed. 60 (1983) 702.